

## Ultrahigh-speed multimodal adaptive optics system for microscopic structural and functional imaging of the human retina: supplement

ZHUOLIN LIU,<sup>1,\*</sup>  FURU ZHANG,<sup>1,2</sup> KELVY ZUCCA,<sup>1</sup> ANANT AGRAWAL,<sup>1</sup>  AND DANIEL X. HAMMER<sup>1</sup> 

<sup>1</sup>Center for Devices and Radiological Health (CDRH), U. S. Food and Drug Administration (FDA), Silver Spring, Maryland 20993, USA

<sup>2</sup>Co-first author

\*[Zhuolin.Liu@fda.hhs.gov](mailto:Zhuolin.Liu@fda.hhs.gov)

---

This supplement published with Optica Publishing Group on 17 October 2022 by The Authors under the terms of the [Creative Commons Attribution 4.0 License](https://creativecommons.org/licenses/by/4.0/) in the format provided by the authors and unedited. Further distribution of this work must maintain attribution to the author(s) and the published article's title, journal citation, and DOI.

Supplement DOI: <https://doi.org/10.6084/m9.figshare.21197824>

Parent Article DOI: <https://doi.org/10.1364/BOE.462594>

# Ultrahigh-speed multimodal adaptive optics system for microscopic structural and functional imaging of the human retina: supplemental document

Zhuolin Liu\*, Furu Zhang†, Kelvy Zucca, Anant Agrawal, and Daniel X. Hammer

*Center for Devices and Radiological Health (CDRH), U. S. Food and Drug Administration (FDA), Silver Spring, Maryland 20993, USA*

*†Co-first author*

*\*[Zhuolin.Liu@fda.hhs.gov](mailto:Zhuolin.Liu@fda.hhs.gov)*

## Supplementary materials

### *Front end optics setup*

The three beams in the system (OCT, SLO, and AO beacon) are combined and coaligned using two high-performance, high efficiency dichroic beam splitters indicated by LP and SP in Fig. 1 (Semrock, Rochester, NY, USA) and a 90/10 beam splitter. The backscattered AO-OCT light is collected with the same launch fiber and interfered with the reference beam in a 50/50 fiber coupler. The interference signals are detected using a balanced detector (PDB481C-AC, Thorlabs), and then digitally sampled using a high-speed digitizer (ATS9373, Alazartech, Pointe-Claire, Canada). The backscattered AO-SLO light is filtered with a spatial pinhole and detected with an avalanche photodiode (APD, C10508, Hamamatsu Photonics K.K., Japan), and digitized with an analog framegrabber (Solios eA/XA quad, Matrox Inc., Montreal QC Canada). The backscattered AO beacon is imaged using a SHWS (30×30 lenslet array, 300- $\mu\text{m}$  pitch; MLA300-14AR-M, Thorlabs). A telescope demagnifies the wavefront sensing beam from 7.4 mm to 6 mm to fit the SHWS camera chip (Pixelink PL-D734, Navitar, Inc., Rochester NY USA).

### *Internal fixation and visible stimulus design*

An organic light-emitting diode (OLED) microdisplay (DSVGA, eMagine, NY USA) is used for internal fixation with a Badal lens relay. The optical setup [1] of the fixation channel allows imaging across a 30° retinal region with -20 to +10 diopter (D) sphere correction range, while providing a long eye relief to allow integration with the AO imaging beams. A stimulus channel is combined with the fixation channel using a 50/50 beam splitter. A SuperK Extreme supercontinuum laser (NKT Photonics, Birkerød, Denmark) is used as a stimulus light source. The wavelength was limited to a 10 nm bandwidth around central wavelengths of 526 nm and 640 nm used for this study by connecting this laser to a SuperK Varia tunable filter. The delivery and synchronization of the stimulus into the eye was controlled by an acousto-optic modulator (AOM, 3080-125, Gooch & Housego LLC, Palo Alto CA USA). The AOM is aligned on a rotary stage so that only the first-order diffracted beam (RF driver high signal) is coupled by a lens into a 200- $\mu\text{m}$  diameter core multimode fiber (FPC-0200-22-10SMA, Mightex Systems, North York ON Canada). The stimulus light is re-collimated after the fiber and limited by an iris aperture to a diameter that subtends 2° on the retina after passing through a dichroic beamsplitter and through the same lens relay as the fixation target into the eye. The stimulus beam is co-aligned to the OCT-SLO raster. The shutter further prevents overexposure by opening only during stimulus acquisition. The stimulus channel uses one of six stimulus band (10 nm bandwidth) from the supercontinuum light source centered at 450, 526, 606, 640, and 660 nm to probe S-, M-, and L- type cone photoreceptors. The AOM was driven by an arbitrary

square waveform, allowing flexible delivery of millisecond pulse durations. The FDML imaging source triggered the AOM drive waveform, ensuring the stimulus pulses were synchronous with the image acquisition.

#### *FDML AO system instrumentation and control software*

Two workstations running Windows 10 and equipped with graphical processor unit (GPU) video cards (GeForce RTX 2080, Nvidia Inc., Santa Clara CA USA) and all system data, signal, and image acquisition boards are used to operate the system. The first computer handles all SLO and OCT image acquisition functions. The second computer handles WS sensing and AO control.

The FDA FDML AO system derives all timing and synchronization from the FDML laser operating at a 3.348 MHz sweep rate. A synchronization signal from the FDML drives the resonant scanner at its designed resonance frequency of 3.348 kHz using a bidirectional 500-pixel scan. Both SLO and OCT beams use the resonant scanner in a simplified arrangement compared to previous multimodal systems that require a minimum of three scanners [2]. The FDML produces a 6.696 kHz horizontal scan synchronization signal (Hsync) that is used to drive the SLO framegrabber and trigger the OCT high speed digitizer. The 3.348 MHz clock from the FDML is sent to the pixel clock of the Alazar digitizer. The FDML also generates a vertical synchronization signal (Vsync) for the Matrox framegrabber and Alazar digitizer, as well as a sawtooth waveform to drive the slow axis galvanometer scanner at 13.4 Hz. In this way, SLO images and OCT volumes, both with 500×500-lateral pixels, are acquired synchronously. A data acquisition board (PCIe-6363, National Instruments Inc., Austin TX USA) is used to acquire the volume synchronization signal from the FDML and to generate analog voltages to drive the RS amplitude, SLO power, and stimulus waveform. The SLO-OCT computer also uses USB ports to interface with the stimulus laser, stimulus optical beam shutter (SH05 and KSC101 compact shutter controller, Thorlabs), and fixation target linear stage (Zaber Technologies Inc., Vancouver BC Canada).

The wavefront sensor and pupil cameras (PixelLink PL-D734MU-NIR, Navitar, Inc.) use the USB3 interface to transfer images to the WS-AO computer. This computer also has a USB-6363 data acquisition board (DAQ, National Instruments Inc.) that generates an analog output voltage to drive the AO beacon power. The pupil is illuminated with a near-infrared LED array with center wavelength at 840 nm. The deformable mirror is controlled by the WS-AO computer via USB interface.

The FDML laser is controlled by software written in LabVIEW by Optores GmbH. Custom software was written to control the SLO-OCT acquisition and all instrumentation (fixation target, stimulus channel, etc.) described above. Some control variables from the Optores software are accessed in the SLO-OCT acquisition software, for example to change the scan amplitude or adjust the phase of the bidirectional scan. Because the SLO images and OCT B-scans are scanned with the RS in a sinusoidal pattern, custom CUDA GPU codes were written to dewarp them for real-time display. Custom CUDA GPU code is also written to produce OCT B-scans for live display from the acquired and digitized spectra using standard OCT processing steps [3].

Custom software was written to control the WS camera, pupil camera, and DM on the WS-AO computer. Custom CUDA GPU code is used to calculate the WS centroids in ~2 ms. The WS images can be acquired at rates up to ~50 fps. Calibrated control code drives the DM actuator values from the WS slopes in a closed-loop manner. For pupils smaller than the designed 7.4-mm beam size, the closed-loop AO algorithm nulls the contribution of SH lenslet slopes that fall outside of the actual pupil to the DM drive signal. The DM actuator map, wavefront aberration map, and Zernike coefficients are also displayed on the user interface in real time.

## Reference

1. Steven S., Sulai Y.N., Cheong S.K., Bentley J., and Dubra A., 'Long eye relief fundus camera and fixation target with partial correction of ocular longitudinal chromatic aberration,' *Biomed Opt Express* **9**(12), 6017-6037 (2018).
2. Liu Z., Tam J., Saeedi O., and Hammer D.X., 'Trans-retinal cellular imaging with multimodal adaptive optics,' *Biomed Opt Express* **9**(9), 4246-4262 (2018).
3. Ustun T.E., Iftimia N.V., Ferguson R.D., and Hammer D.X., 'Real-time processing for fourier domain optical coherence tomography using a field programmable gate array,' *Rev Sci Instrum* **79**(11), 114301 (2008).

## Supplementary Figures

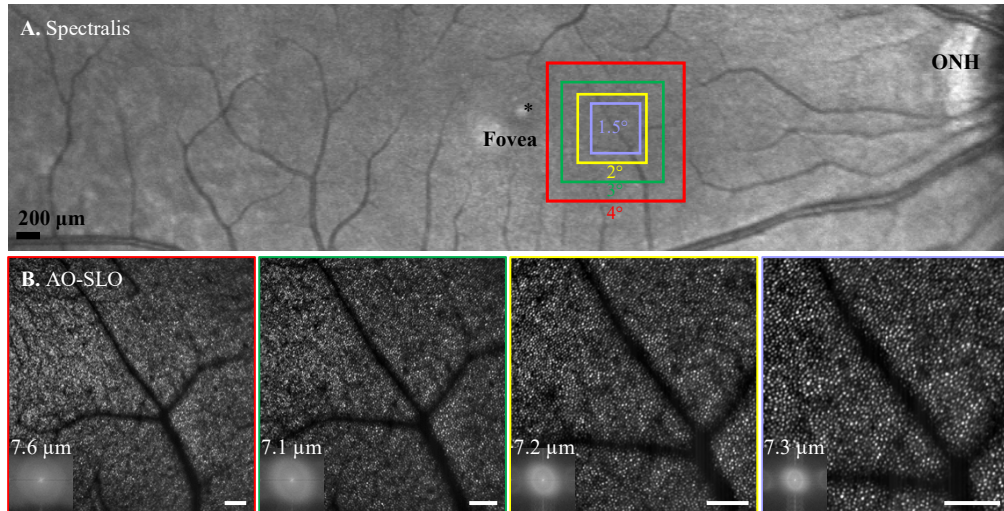


**Fig. S1.** **A.** Spectralis macular scan. **B.** Representative wide field cone images of S1 collected at 3° nasal retinal location with the FDA FDML-AO system. Color coded AO-SLO images (from left to right) with 4°, 3°, 2° and 1.5° square field size. Insets show the power spectra of the corresponding images. The Nyquist limit is 4.8 μm, 3.6 μm, 2.4 μm and 1.8 μm for the four scans. The scale bar in **B** is 100 μm.

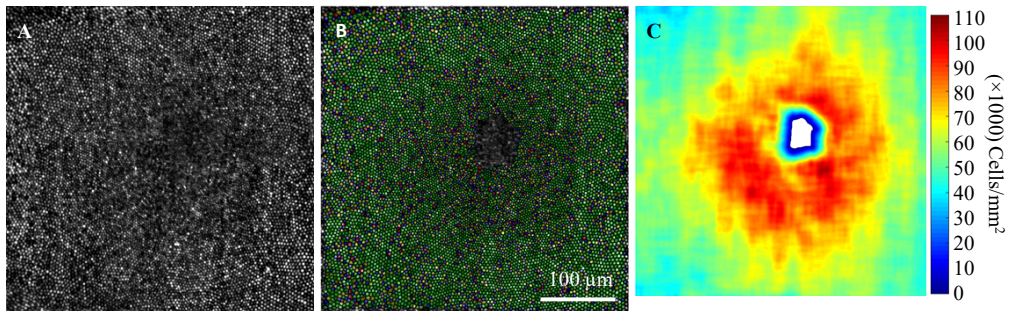


**Fig. S2.** Representative foveal cone mosaic of S1. **A.** Montage of four AO-SLO scans with 0.75°x0.75° FOV show cones are resolved everywhere except for a 50-μm region at the fovea center. **B.** The corresponding Voronoi map is superimposed on cone image in **A.** for cell density calculation which is defined as the ratio of total number to total area of the Voronoi patches. Color key for number of nearest neighbors is: purple: 4, blue: 5, green: 6, yellow: 7, and red: 8. **C.** Heat map shows the cone density monotonically decreases with increasing distance from the center fovea.

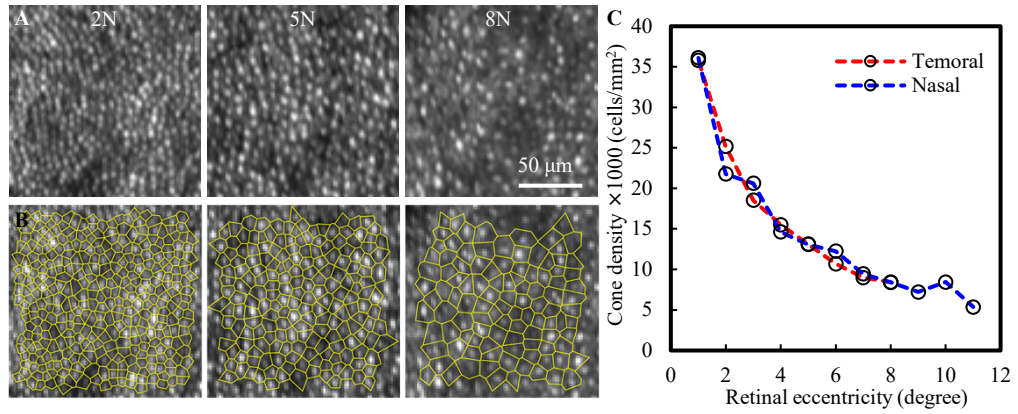


**Fig. S3.** Cone density as function of retinal eccentricity quantified from Fig. 6. **A.** Representative AO-SLO images at 2°, 5° and 8° nasal to the fovea and their corresponding Voronoi maps for density calculation in **B.** **C.** Plot of cone density.

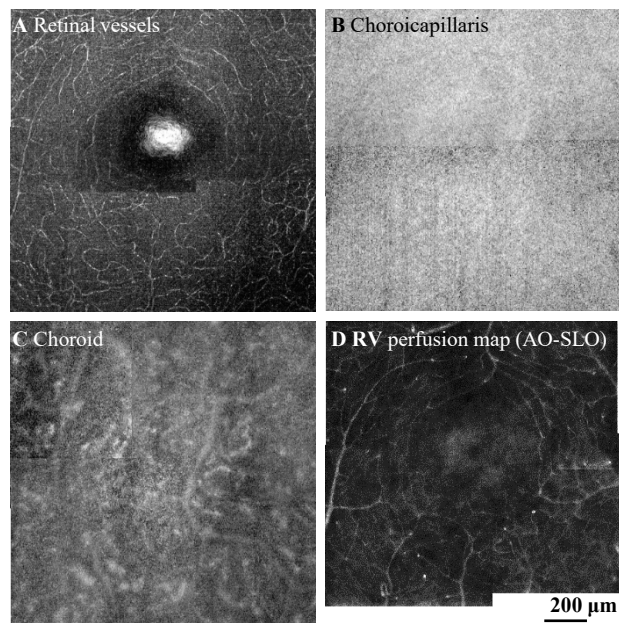


**Fig. S4.** AO-OCT imaging at the fovea of S1 with four 3°×3° FOV scans. AO-OCT intensity *en face* projections at the depth of **A.** retinal vessels (RV), **B.** choriocapillaris, and **C.** choroid. **D.** AO-SLO perfusion map reveals retinal vessels at fovea.

## Supplementary Tables

Table S1. FDA FDML AO system sample arm design parameters

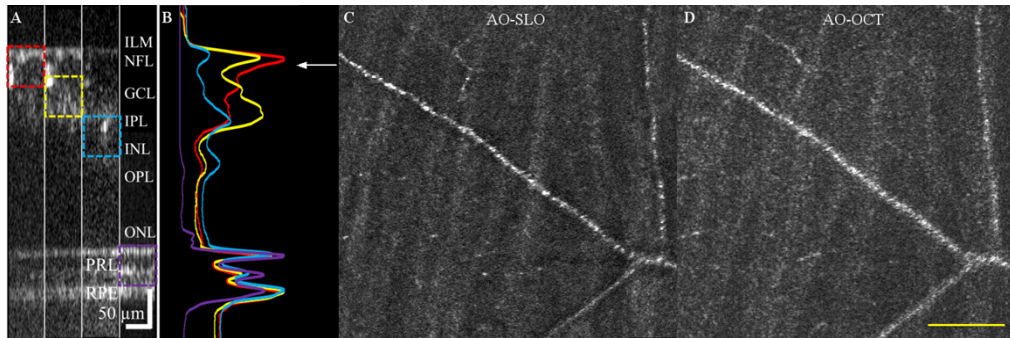
Optical element	$f$ (mm)	$I_x$ (deg)	$I_y$ (deg)	$D$ (mm)
<b>Imaging Beam</b>				7.4
<b>SM1</b>	500	0	2.92	
<b>SM2</b>	500	2.92	0	
<b>RS</b>		-6	0.17	7.4
<b>SM3</b>	500	2.39	2.39	
<b>SM4</b>	500	-2.39	2.39	
<b>G</b>		5.3	0.04	7.4
<b>SM5</b>	500	-2.4	-3.36	
<b>SM6</b>	900	4.5	-3.22	
<b>DM</b>		-5	-0.07	13.3
<b>SM7</b>	900	2.2	3.57	
<b>SM8</b>	500	-2.68	1.65	
<b>Eye pupil plane</b>		-	-	7.4

Table S2. FDA FDML multifunctional and multimodal imaging parameters

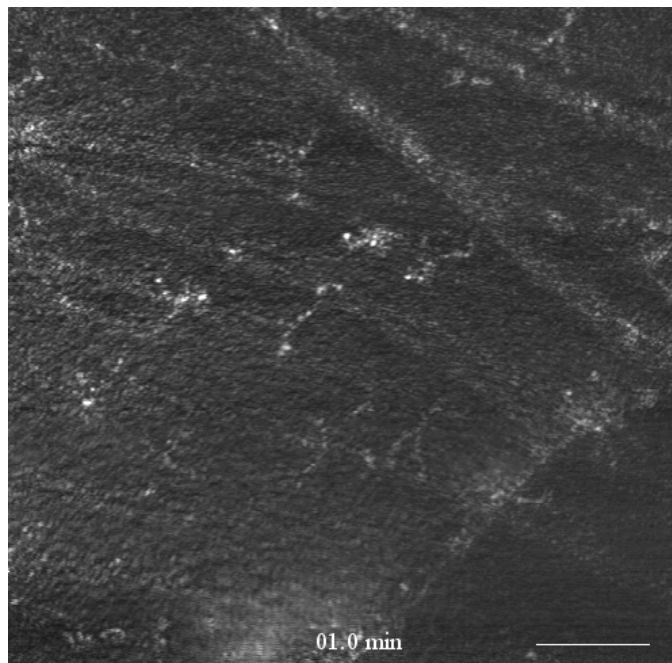
Protocol	FOV (°)	Retinal Location (°)	Number of videos	Volumes/video	Lateral sampling ( $\mu\text{m}/\text{pixel}$ )	Volume rate (Hz)
<b>1. Inner retina</b>	2°×2°	10°T	20	15	1.2	13.4
<b>2. Outer retina</b>	1.5°×1.5°	3°T	10	19	0.9	13.4
<b>3. Wide field</b>	4.5° × 4.5°	12°N to 12°T	1	15	2.7	13.4
<b>4. Cone function</b>	1.5°×1.5°	3°N	16	15	0.9	13.4
<b>5. OCTA</b>	3°×3°	-11°N to 11°T	1	1	2.4	1.675

Note: N: nasal; T: temporal; OCTA: optical coherence tomography angiography

## Supplementary Visualization



**Visualization 1.** A shows the averaged of 15 AO-OCT B-scans along the slow scan direction, the image are stitched from four sub-images that were acquired with system focus at the four primary depths from the same retinal location. The color-coded dash boxes represent the ranges for generating the corresponding AO-OCT *en face* images in D. B shows the averaged A-scan profiles respect to the four system focuses. Co-registered averaged 1.5° FOV retinal images from S1 for simultaneous AO-SLO (C) and AO-OCT (D) with the system focus set approximately at four depths (ILM-GCL: frame 1-15; GCL-IPL: frame 16-30; IPL-OPL: frame 31-45 and PRL: frame 46:60) which are indicated as the white arrow in B. The AO-SLO data were collected with a one Airy disk diameter (ADD). The AO-OCT *en face* images were created by the amplitude projection of a AO-OCT 50 μm slab through the system depth of focus. Scale: 100 μm.



**Visualization 2.** A time-lapse video was created for tracking the movement of macrophage processes at 10° temporal to the fovea from subject S1. Scale: 100 μm